Methodology for developing models to estimate vehicle instantaneous energy consumption based on hub-type dyno test data

Amati Nicola [1], Castellanos Molina Luis Miguel [1], Mancarella Alessandro [2], Marello Omar(*) [2] and Silvagni Mario [1]

[1] *Center for Automotive Research and Sustainable Mobility (CARS), Department of Mechanical and Aerospace Engineering (DIMEAS), Politecnico di Torino, Corso Duca degli Abruzzi 24, 10129, Italy.*

[2] *Center for Automotive Research and Sustainable Mobility (CARS), Department of Energy (DENERG), Politecnico di Torino, Corso Duca degli Abruzzi 24, 10129, Italy.*

(*) Corresponding author. E-mail: omar.marello@polito.it

Methodology for developing models to estimate vehicle instantaneous energy consumption based on hub-type dyno test data

Abstract

This paper describes a methodology to develop simple energy consumption models of road vehicles exploiting transient experimental datasets obtained from a vehicle/powertrain four-dyno testbed available at the Center for Automotive Research and Sustainable mobility (CARS@POLITO) of Politecnico di Torino. These models, based on a locally weighted linear regression method, can serve as a simpler alternative to more conventional methods based, for example, on engine maps obtained by steady-state characterization at engine testbeds, and combined with powertrain subsystem models. The present methodology was applied to a conventional diesel-powered vehicle. Three different modelling approaches are proposed: vehicle-based (VB), engine-based (EB) and engine-based modified (EB*). The VB approach is the simplest, being able to estimate the vehicle fuel consumption by only using, as inputs, wheel torque and speed, while the EB and EB* approaches enhance modelling accuracy by using engine speed and torque, as inputs, along with transmission-related parameters and/or by considering the moments of inertia of the powertrain rotating parts. The manuscript describes, in full, the process used to develop these models, providing significant guidance for researchers who may want to replicate the procedure with their own experimental data. These energy consumption models can be useful tools for the development and assessment of eco-driving or ADAS functions or for energy consumption comparison between different vehicles that were not tested on the same driving cycle. They can also support the estimation of the total energy consumption of vehicles along different traffic conditions or routes, based on a limited number of experiments and low computational effort.

Keywords: energy consumption models, road vehicles, powertrain testbed

1. Introduction

In a global context of dwindling natural resources, climate change and urban air pollution, governments around the world are pushing towards more energy efficiency and less polluting road vehicles. Concretely, more efficient internal combustion engines (ICEs) and electric motors (EMs), eco-driving and eco-routing controls, advanced driver assistant systems (ADAS) and new primary energy sources, are all topics researchers are investigating thoroughly to limit the impact of the road

transport sector on the environment. For some of these topics, e.g. in order to develop and evaluate ADAS algorithms [1], in-vehicle eco-driving assistants or to create eco-routing simulators, suitable vehicle modelling methodologies are crucial to correctly predict instantaneous energy consumption [2,3].

Energy consumption is extremely dependent on the vehicle power demand (VPD). Thus, any reliable vehicle model that attempts to predict instantaneous energy consumption, requires, even in a simplified 1-D longitudinal dynamic model, vehicle data (e.g, equivalent mass) and input variables such as vehicle velocity, road grade and road load coefficients, which are all essential to estimate the instantaneous VPD. Then, depending on the amount of further data required to be built and to its transparency to the vehicle being modelled, a vehicle model for energetic analyses may be classified into one of the following broad categories: white-box, grey-box and black-box models [4,5]. White-box models are highly deterministic and require a thorough understanding (and associated expertise) of each sub-component included within the entire vehicle system [6]. Many input parameters (such as ICE/EM characteristics, masses, moments of inertia, gearbox frictions, auxiliary power, and so on) need to be included into the resulting sub-models, despite many of these parameters are either difficult to measure or impossible to obtain from the OEMs due to property barriers [7]. A black-box model, in contrast, lacks physics-based knowledge in the model structure and just employs an input-output data scheme (to be derived from experimental campaigns) to estimate energy consumption, giving the possibility to build a much more readily available model. Grey-box models fit in between: they are built combining some insight into the system with empirical data obtained from experiments [8].

With a black-box modelling approach, just the ICE/EM (i.e., the prime mover) is usually regarded as a black box [4]. For a conventional ICE-powered vehicle model, for instance, engine-level variables, such as engine rotational speed and torque, are typically used as inputs to engine-based fuel consumption models, which are, in most cases, represented as simple steady-state engine maps that need to be experimentally measured at dedicated engine testbeds. When engine fuel

consumption estimation is performed with this approach, polynomial regression is typically used. Unfortunately, steady-state polynomial functions usually present a challenge in capturing system transient behaviours while maintaining model simplicity. In general, steady-state fuel consumption models alone are inadequate for actual transient driving conditions [9].

One way to include transient effects into engine fuel consumption estimation is to apply transient corrections to steady-state engine maps, and several examples can be found in the literature [10,11] in this regard. This approach, referred to as "transient-correction-based", determines the steady-state engine fuel consumption by using engine speed and torque, and then modify the results by introducing transient correction. For example, Chiara et al. [10] developed an instantaneous fuel consumption model of a diesel engine characterized by several sub-modules that generate correction factors based on the engine intake airpath dynamics. Instead, Lindgren [11] developed a semi-static model extended with transient correction factors that accounted for both changes in engine speed and torque, for the estimation of the fuel consumption of an engine of a non-road mobile machinery.

Besides the simplicity of these approaches, longitudinal dynamics equations need to be coupled with these engine fuel consumption models through the addition of extra sub-component models of the entire vehicle driveline, requiring rather detailed knowledge of all of them [12].

Another way to tackle the problem of instantaneous fuel consumption estimation is to exploit machine-learning techniques, such as artificial neural networks (ANNs) [13]. Machine-learning approaches typically use, as inputs, vehicle-level variables such as vehicle velocity and wheel torque, without the need to detail each sub-components of the entire vehicle powertrain [14]. Fuel consumption models based on machine learning methods can yield higher accuracy and faster computing speed. For example, Mortabit et al. [15] developed an instantaneous vehicle fuel consumption estimation method using Long Short-Term Memory Neural Networks (LSTMs). The model prediction error was around 8% of fuel consumption and the R^2 was 0.97.

However, such models need vast experimental datasets for model training (based on the assumption of sufficiently high computational power available), and a significant amount of time to calibrate the data. Moreover, these models may only be applicable within a certain range and their ability to predict beyond that range is generally uncertain [16].

To address the limitations of the aforementioned approaches based on steady-state engine maps or machine learning, this paper investigates how a locally weighted linear regression method can be used to create simple models for predicting of the instantaneous fuel consumption of a conventional diesel-powered vehicle. First, a simple vehicle-based black-box model, which does not require any engine- or transmission-related data, is built from a small set of transient experimental data (such as type-approval or real-driving cycles) collected on a vehicle/powertrain testbed. Valuable insight is given into how to improve this simple vehicle-based fuel consumption model by properly handling training data and by adding to the model few easily available internal system variables (such as engine speed and engaged gear), thus investigating improved grey-box modelling approaches. The methodology is intended to give basic support for building similar models for any other vehicle (ICE-powered, hybrid or electric) with a small amount of experimental data gathered at the testbed, no need of detailed vehicle sub-components specifications and modeling, while providing a satisfactory level of accuracy and requiring limited computational power. The possibility of using experimental measurements from one particular test cycle to predict the fuel consumption over another cycle will be demonstrated.

The value of the proposed method lies on the potential for the use of such relatively simple vehicle-level energy consumption models to develop and assess eco-driving, eco-routing or ADAS controls, and to allow the comparison of the energy consumption between two different vehicles that were not tested on the same driving cycle. These models can also provide valuable support to estimate the total energy consumption of the same type of vehicle fleets for different traffic conditions or routes, and to provide a better assessment of the use-phase energy consumption of a vehicle for LCA analysis, based on a limited number of experimental measurements performed

during laboratory testing. To carry out such types of assessments, only vehicle velocity profiles need to be defined. Then, wheel torque can be estimated through coast-down coefficients to serve as second input to the fuel consumption models.

2. Experimental setup

Data reported in this study were gathered from the vehicle and powertrain testbed of the Center for Automotive Research and Sustainable mobility (CARS) Laboratory, at Politecnico di Torino (Italy). The tested vehicle (whose main technical specifications are listed in **Table 1**) was a light-duty commercial vehicle (IVECO Daily), rear-wheel driven, with automatic transmission, equipped with a 2.3 l Euro 6d-temp diesel engine.

Table 1: Main vehicle data.

Vehicle Specifications	
Engine type	2.3-l diesel Euro 6d-temp
Number of cylinders	4
Max. engine power	100 kW @ 3250 rpm
Max. engine torque	390 Nm @ 1500 rpm
Transmission type	Automatic
Top gear number	8
Wheel radius	0.361 m
Equivalent mass	3283 kg
Coast-down (road test) coefficients	$f_0 = 345$ N; $f_1 = 0$; $f_2 = 0.1007$ N/(km/h)^2
Coast-down (dyno) coefficients	$f_0 = 275$ N; $f_1 = 0$; $f_2 = 0.1003$ N/(km/h)^2

2.1. Experimental facility

The vehicle and powertrain testbed is equipped with four independent hub-type dynamometers (AVL DynoULTRA PMM 2500), connected to the front and rear axles of the tested vehicle (each dyno needs to be connected to each of the four wheel hubs with purposely manufactured adapter flanges after removing the wheels), allowing the simulation of road load resistance such as uphill, downhill, rolling resistance, and aerodynamic drag along type-approval and custom driving cycles. Each dyno has a nominal torque of 2500 Nm, nominal power of 260 kW and maximum speed of 3000 rpm. A wind blower put in front of the vehicle follows the vehicle velocity profile (up to 180 km/h) second-by-second in order to provide representative cooling to the vehicle radiator,

reproducing real-life operation.

An automatic gear-shifting and pedal-actuating robotized driver (Stähle Autopilot SAP2000), visible in **Figure 1**, was used to automatically perform start-up and stop maneuvers onboard the vehicle during testing, as well as to select the available driving modes of the vehicle automatic transmission (park, neutral, driving). The robot is made up of three mechanical legs (an accelerator leg, a brake leg, and a clutch leg), and a shifting arm connected to the gearshift lever. To ensure maximum repeatability, the accelerator pedal was handled directly from the testbed automation through analog signals, bypassing the physical pedal, whereas the brake mechanical leg was connected to the corresponding pedal only to perform correct start-ups. This is because hub-type dynamometers can simulate the longitudinal load transfer during both accelerating and braking phases. Therefore, braking maneuvers can be performed directly by imposing the proper braking torque to the dynos, completely removing the braking pads from the brake calipers to avoid damaging dyno magnets with any harmful particle emission.

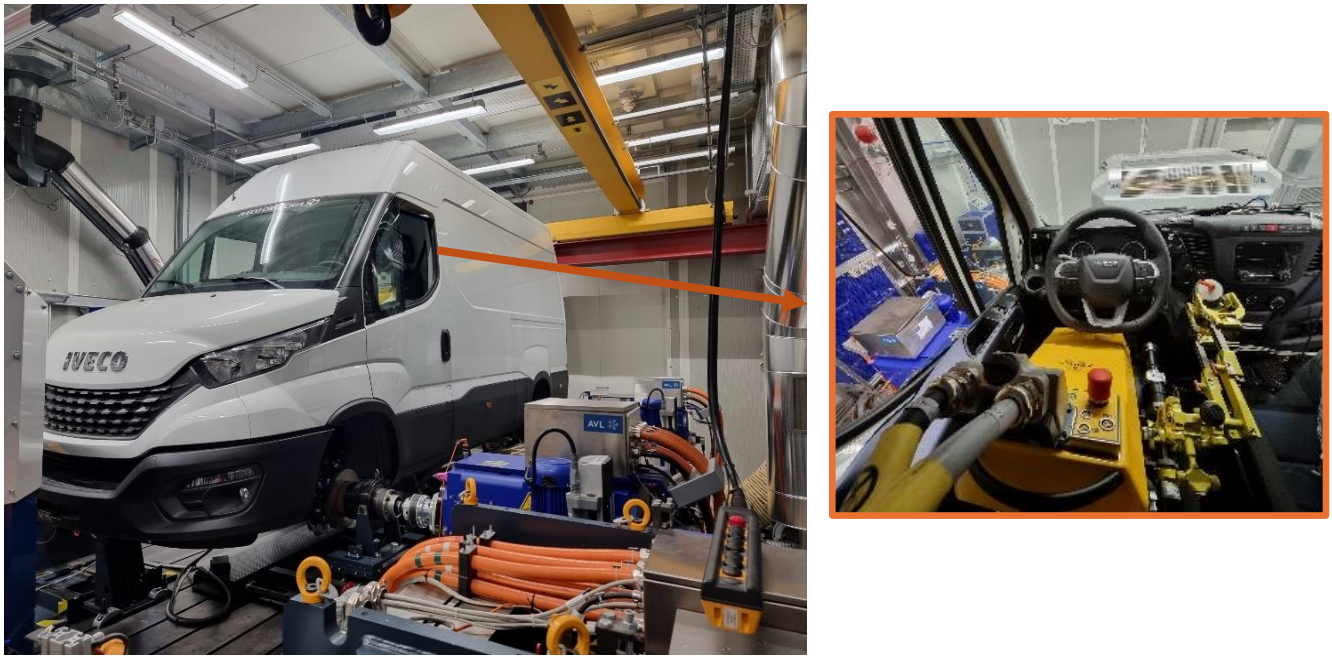

Figure 1: Left picture:Vehicle installed in the experimental facility. Right picture: Robotized driver placed in the driver's seat.

Upon vehicle installation, and based on the available experimental results of a coast-down test conducted on a test track using the same tested vehicle, the dynamometer load adaptation procedure was performed: the coast-down coefficients (f_0, f_1, f_2, cf. **Table 1**) in the automation software were tuned in order to obtain the same deceleration time for the vehicle velocity interval (0-130 km/h) as measured during the coast-down test.

2.2. Measurement equipment and signals

While there were many measurement signals available, only a selected handful, such as wheel rotational speed, wheel torque, and instantaneous fuel mass flowrate, are crucial for building vehicle-level fuel consumption models. All of these signals (listed in **Each hub-type** dynamometer is capable of independently measuring the wheel rotational speed and torque. High-frequency rotational speed signals are available through four built-in shaft position encoders (Heidenhain ROC 413-2048), which are needed for closed-loop speed control of the dyno motors, while four HBM T12HP flange-type torque transducers (accuracy class 0.02, nominal torque 5 kNm) provide accurate wheel torque measurement. No direct engine torque measurement is available, neither from testbed equipment nor from on-board diagnostics (OBD) signals.

Table 2) were measured either directly from the testbed equipment (e.g., dynamometers, fuel consumption measurement device, etc.) or from the vehicle itself.

Each hub-type dynamometer is capable of independently measuring the wheel rotational speed and torque. High-frequency rotational speed signals are available through four built-in shaft position encoders (Heidenhain ROC 413-2048), which are needed for closed-loop speed control of the dyno motors, while four HBM T12HP flange-type torque transducers (accuracy class 0.02, nominal torque 5 kNm) provide accurate wheel torque measurement. No direct engine torque measurement is available, neither from testbed equipment nor from on-board diagnostics (OBD) signals.

Table 2: Noteworthy measurement signals recorded in the data-logging process.

Signal	from Testbed	from Vehicle
Wheel rotational speed	Available	n/a
Vehicle velocity	Available	Available
Engine rotational speed	n/a	Available
Wheel torque	Available	n/a
Fuel mass flowrate	Available	n/a
Accelerator pedal position	Available	Available
Current gear	n/a	Available

For fuel consumption, the engine fuel supply and return lines were connected to the AVL FuelExact device (FuelFlex version, suitable also for alcohol admixtures and up to 100% biodiesel), available in the testing facility and able to provide precise and continuous fuel consumption measurement with a 0.1% uncertainty (according to DIN 1319) within a range up to 500 kg/h. Conventional diesel fuel with up to 7% biofuel (B7), in keeping with the European EN 590 standard, was used for all tests.

All of the abovementioned equipment and measurement devices are controlled by the automation system AVL PUMA 2.

2.3. Experimental test description

For the purpose of this study, the vehicle was tested along four different transient driving cycles:

1. the Worldwide harmonized Light-duty Test Cycle (WLTC);
2. the US EPA Federal Test Procedure driving cycle (FTP-75);
3. a cycle comprising two Transport for London Urban Inter-Peak (TfL UIP) plus a final custom driving profile, representative of motorway driving conditions (henceforth referred to as “RDE”);
4. a custom driving cycle representative of rural driving conditions (henceforth referred to as “Rural”).

A fifth custom test, henceforth referred to as “Steady-states” (SS), was also carried out by simulating different road gradient steps while varying the accelerator pedal position (APP) from a

minimum value (the bare minimum to keep the vehicle at a stop) to 100% and waiting the vehicle to reach quasi-steady state conditions at each APP step. In details, starting with a flat road (0% road gradient), the APP was varied in 10% increments from 0% to 100%. Subsequently, the road gradient was increased by 5% and the APP sweep was repeated again from a minimum value, needed to prevent the vehicle from moving backwards, to 100%. This procedure was performed up to 30% road gradient (in 5% road gradient increments), since the vehicle was not able to overcome resistances given by this slope value. The vehicle velocity profiles of each of these five tests are showed in **Figure 2**.

Finally, an additional dataset referred to as "Joined" will be utilised; it comprises all of the aforementioned tests in a single dataset.

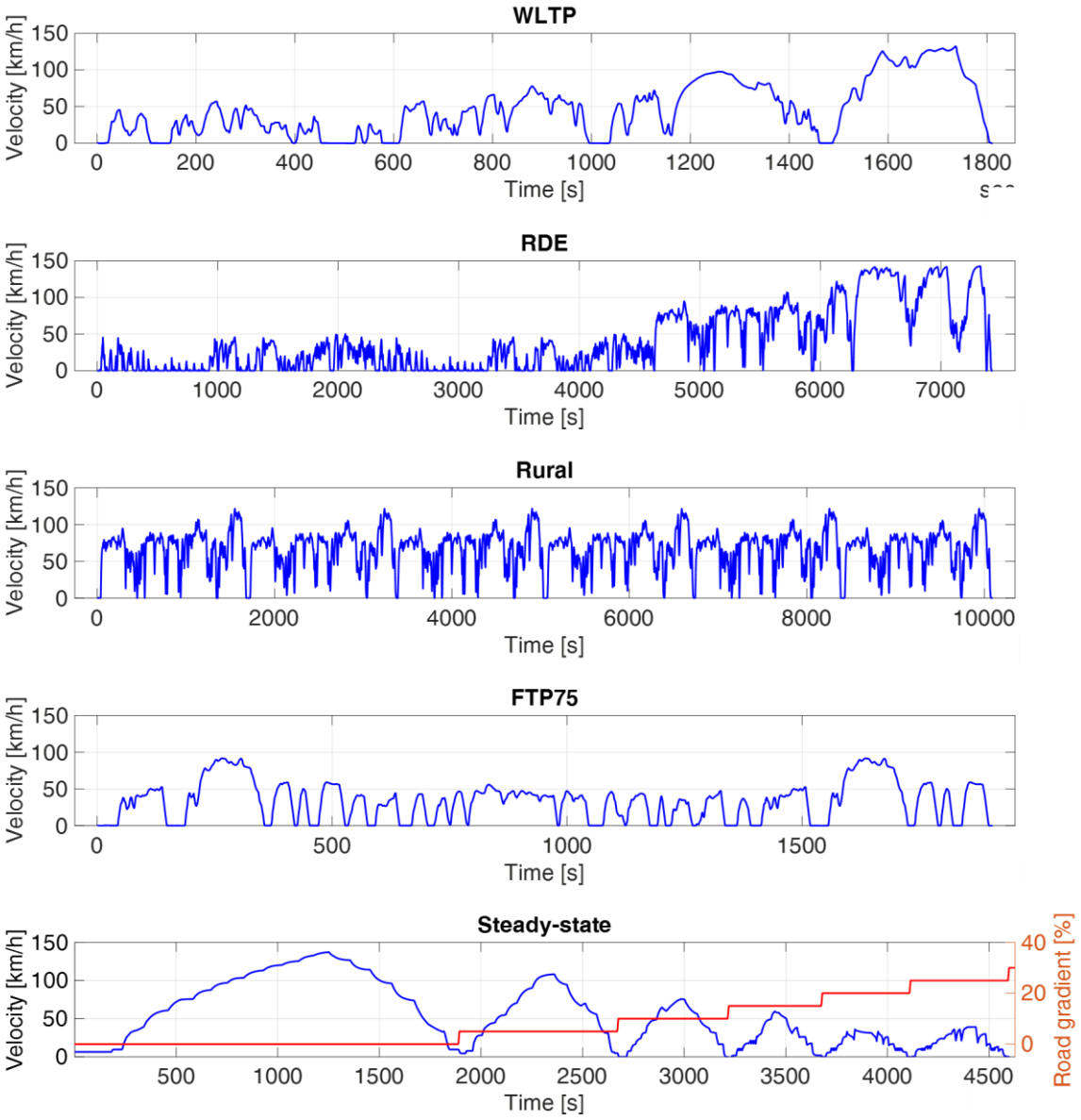

Figure 2: Vehicle velocity profiles along the considered driving tests.

All the tested driving cycles were started with the vehicle already in warmed-up conditions. The testbed was conditioned at ambient temperature of 25 °C, while no humidity control is provided.

3. Methodology

As previously stated, the goal of this study is to generate rather simple, easy-to-use, straightforward models to estimate vehicle fuel consumption based on measurement datasets coming from the experimental facility described in **Section 2**. To achieve this goal, proper interpolating functions, which can potentially be converted into maps, were generated by means of the Curve Fitting

Toolbox software in MATLAB, employing a “lowess” approach (“lowess” stands for “locally weighted scatter plot smooth”) that smooths experimental data using a locally weighted non-parametric regression method. Similarly to a moving average approach, this smoothing process is local since every smoothed value is determined from neighbouring data within a locally weighted span, without explicit mathematical expression on the global domain.

Figure 3 depicts a flowchart representation of the main methodology steps followed in the present study.

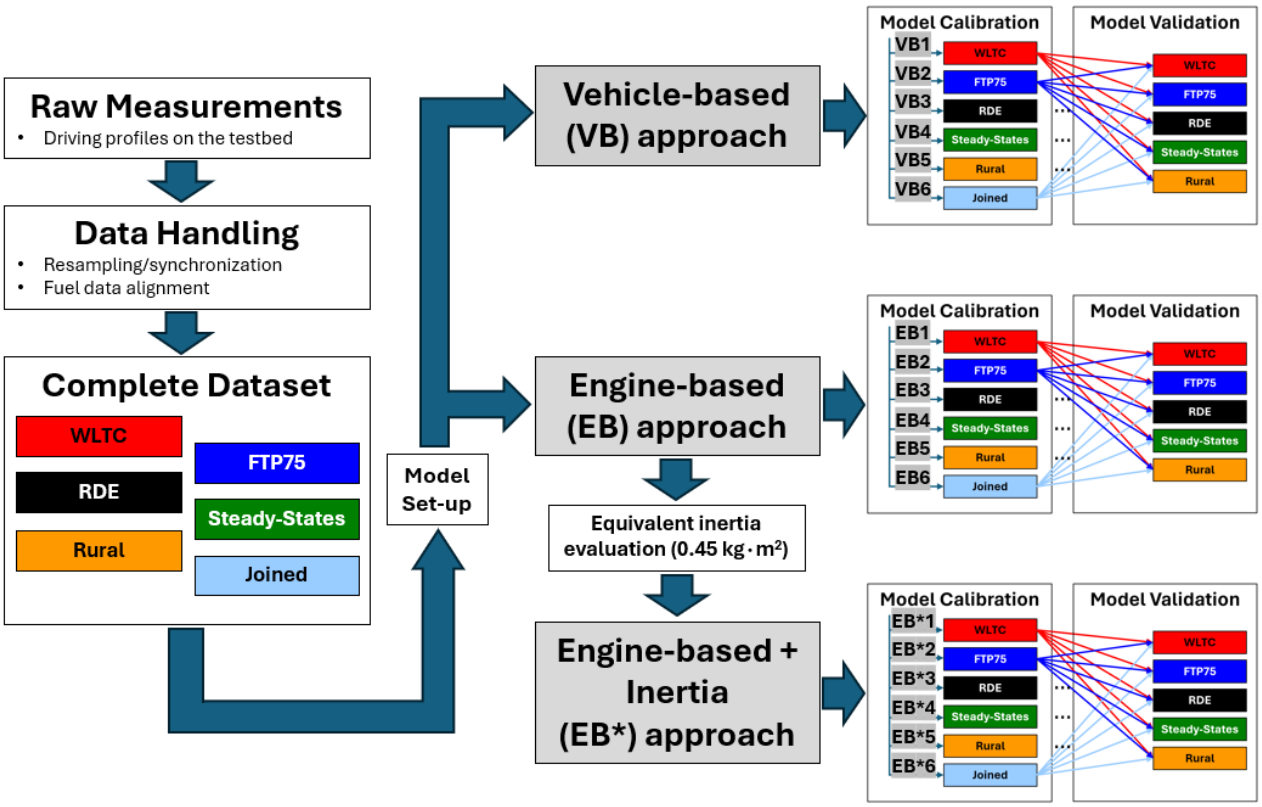

Figure 3: Flowchart representation of the main methodology steps.

First of all, a raw dataset was generated by including all the relevant measurement signals coming from the testbed facility and the vehicle. Since all these signals come from different devices and/or communication channels, they typically have different sampling frequencies, thus needing a first resampling procedure. A second issue was that fuel consumption measurements, for reasons that will be detailed in **Section 4.5**, were not perfectly synchronized with speed and torque values, thus needing a synchronization procedure as well. After these issues were properly tackled, the complete dataset was ready for model set-up. Distinct modelling approaches were investigated and

will be referred to as “VB” (vehicle-based), “EB” (engine-based) and “EB*” (engine-based + moments of inertia).

The simplest black-box model that can be thought of is based on a “VB” vehicle-based approach (cf. **Section 4.2** for detailed information). This model just requires three measurement signals to be calibrated: wheel speed and torque values, which serve as inputs to such model, and instantaneous fuel consumption, which represents its intended output, i.e. the variable that needs to be estimated. In case of electric or hybrid vehicles, also the instantaneous DC electrical power would be required, instead or in addition to the fuel consumption. Then, if additional signals are available, such as engine speed, engaged gear, or instantaneous gear ratio, different types of grey-box models can be investigated, namely “EB” and “EB*” (cf. **Sections 4.3** and **4.4** for detailed information), with the aim of obtaining more precise and/or more consistent fuel consumption estimations.

For each of the considered modelling approaches, several model calibrations (e.g., VB1, VB2, VB3, …; EB1, EB2, EB3, …; EB*1, EB*2, EB*3, …; cf. **Figure 3**) were generated by fitting interpolating functions to each of the experimental driving cycles listed in **Section 3**. Then, to properly assess model performances, each model calibration was used to estimate fuel consumption along all the driving cycles (excluding the “Joined” dataset), i.e., a cross-validation analysis was carried out.

When generating the different model calibrations, a small number of experimental samples was discarded from the calibration datasets: for example, the samples with a vehicle velocity lower than 2 km/h or with a negative wheel torque (in order to avoid interpolation issues due to engine idling or cut-off strategies during braking) and/or with negative values of fuel consumption (brief moments when the fuel mass flowrate device gives negative values are possible due to fuel accumulation phenomena linked to the fuel return line and the flexibility of the hoses connecting the AVL FuelExact device and the engine).

Similarly, for cross-validation, the model calibrations were used to estimate fuel consumption along entire driving cycles, except for operating points where the fuel injection is cut

off or the engine is idling. To avoid any issues with these points, the estimated fuel consumption was set to zero whenever the wheel torque was negative or to idle consumption whenever both the APP was released and the engine rotational speed was lower than a certain threshold, close to idle speed (idle speed + tolerance).

4. Model Creation

4.1. Selection of model inputs

As previously stated, although the objective of the study is to develop fuel consumption models for the whole vehicle/powertrain, these models can be generated as a function of different input variables. For model inputs selection, vehicle-based or engine-based approaches can be adopted. The most readily-available option is to use the rotational speed and torque data recorded at the wheels of the vehicle as input variables ("VB" vehicle-based approach), which are directly measured from the flange-type torque transducers at each hub-dyno.

Alternatively, an "EB" engine-based approach can be used. This involves converting the rotational speed and torque signals measured at the wheels to the engine level, by taking into account the total transmission ratio (engaged gear + differential). It is crucial to understand that this process just applies a model input conversion. This way, although the resulting fuel consumption model takes as inputs engine speed and engine torque values, it should not be misconstrued as a conventional ICE map obtained directly from an engine testbed (with fuel consumption measurements including just engine losses). In our case, fuel consumption measurements that are used to calibrate all the models (including "EB" models) contain all the losses related to the whole powertrain (not only engine, but also gearbox, differential, etc.).

Figure 4(a) depicts the distribution of the experimental points covered with an RDE cycle in the vehicle-based (VB) coordinates domain, while **Figure 4(b)** depicts the same experimental points converted into engine-based (EB) coordinates. As can be seen, despite the fact that the

experimental points were collected through transient tests, they adequately cover the whole working area of the vehicle and engine, respectively.

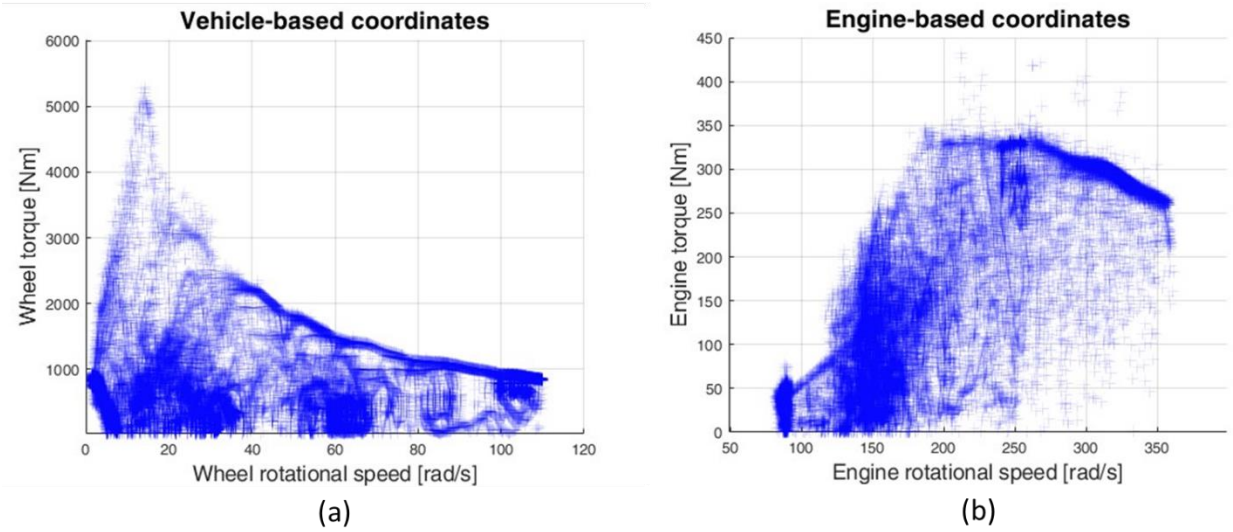

Figure 4: Representation of the operating point distribution in vehicle-based coordinates (a) and engine-based coordinates (b), explored along an RDE cycle.

4.2. Vehicle-based (VB) approach

VB models have the considerable advantage of requiring just three sets of directly measured variables: wheel torque and speed values as inputs, fuel consumption as an output. The downside is that they are completely blind when it comes to the engine operating condition. In other words, given a wheel speed and wheel torque coordinate pair (in the vehicle-based domain), the engine may run at different operating conditions depending on the gear engaged. Therefore, multiple fuel consumption values can be associated with the same wheel speed and wheel torque coordinate pair, potentially resulting in noisier dataset distributions that are more difficult to fit.

4.3. Engine-based (EB) approach

A coordinate transformation from vehicle-based to engine-based can be beneficial to the fitting process, since it allows fuel consumption data, measured at the vehicle level, to be spread in a more relevant domain (engine speed and torque), which has a more direct correlation with fuel

consumption than vehicle operating conditions (wheel speed and torque).

For the purpose of coordinate transformation, depending on the vehicle/engine data available at the testbed, there are several options for obtaining engine-based inputs.

When it comes to determining the engine speed, this can be done either indirectly (by estimating it) or directly (by measuring it). For indirect estimation, the wheel speed needs to be multiplied by the overall instantaneous gear ratio, which depends on the final drive ratio, the instantaneous gear engaged and any other element that can affect the driveline transmission, e.g., for the tested vehicle, the torque converter of its 8-speed automatic transmission, which adds non-negligible complexity to this approach. When no detailed knowledge about transmission is available, indirect estimation of the engine speed may worsen the overall accuracy of the resulting EB model and direct measurement should be preferred. Engine speed, in fact, can be typically retrieved from the electronic control unit (ECU) of a vehicle using the OBD protocol [17]. Using directly measured engine speed data to calibrate EB models yield the most accurate results in terms of fuel consumption, especially during shifting manoeuvres; hence, in this study, engine-based models will be calibrated using direct engine speed measurement.

When it comes to determining engine torque, direct engine torque measurement was not available, neither it is a signal that can be retrieved with appropriate accuracy from the OBD. Consequently, the only viable approach was to use the wheel torque measurement signal and divide it by the overall instantaneous gear ratio, which was evaluated based on the instantaneous gear engaged and the final drive ratio but disregarding any contribution from the unknown torque converter operation.

Once engine speed and engine torque inputs were properly determined, they were used to generate multiple EB models calibrations, one per each considered driving cycle.

4.4. Modified engine-based approach (EB)*

Additional investigation was performed to figure out whether fuel consumption estimation could be

further enhanced. Given that the objective of the study is to calibrate models able to estimate fuel consumptions along transient driving cycles, taking into account the moment of inertia of the powertrain rotating masses into the procedure was the next step (cf. **Figure 3**).

Specifically, starting from an engine-based approach, the moments of inertia can be considered using the formulation reported in **Equation (1)**:

$$T_{engine} = \frac{T_{wheel}}{\tau_{gear} \cdot \tau_{fd}} + J_1 \cdot \frac{dn_{engine}}{dt} + \frac{J_2}{\tau_{gear} \cdot \tau_{fd}} \cdot \frac{dn_{wheel}}{dt} \quad (1)$$

where T_{engine} is an engine-related torque value, T_{wheel} is the measured wheel torque, n_{engine} and n_{wheel} are engine and wheel rotational speed values, respectively, τ_{gear} and τ_{fd} are engaged gear ratio and final drive ratio, respectively, J_1 and J_2 are the moments of inertia corresponding to the masses rotating at engine speed and at wheel speed, respectively.

If moments of inertia data are available for the vehicle under test, **Equation (1)** can be directly used to determine the engine torque for model input. However, since the approach of this study is to develop a viable methodology to build models to estimate fuel consumption without detailed knowledge of the entire powertrain (whose detailed technical specifications, such as moments of inertia, may well be unavailable), a preliminary investigation was followed in order to find out whether there are any feasible ways to obtain reasonable values for moments of inertia directly from the available experimental tests. First, a sensitivity analysis was carried out to assess the influence of J_1 and J_2 on the estimating performance of the resulting models. To do so, J_1 and J_2 were varied over wide ranges (spanning a full-factorial distribution), and for each (J_1, J_2) value pair, a tentative model was calibrated on each available dataset by using the engine torque input that results from **Equation (1)**. The resulting tentative models were then validated (on the same corresponding datasets) to figure out which value pair (J_1, J_2) gave the best estimating performance, as assessed by R^2 (coefficient of determination) and RMSE (Root Means Square Error) statistic measures. The first outcome of this analysis was that J_1 had a substantial impact, whereas J_2

contributed to a negligible extent. Therefore, **Equation (1)** was simplified to **Equation (2)**, i.e., J_2 contribution was neglected:

$$T_{engine} = \frac{T_{wheel}}{\tau_{gear} \cdot \tau_{fd}} + J_1 \cdot \frac{dn_{engine}}{dt} \quad (2)$$

With this simplification, EB* models were calibrated using, as torque input, the result of **Equation (2)**, considering J_1 values spanning a [0, 1] kg·m^2 interval, in 0.025 kg·m^2 increments. The resulting models were then tested on the same datasets. **Figure 5** depicts the results of this analysis, with fuel consumption R^2 and RMSE trends as a function of J_1 values.

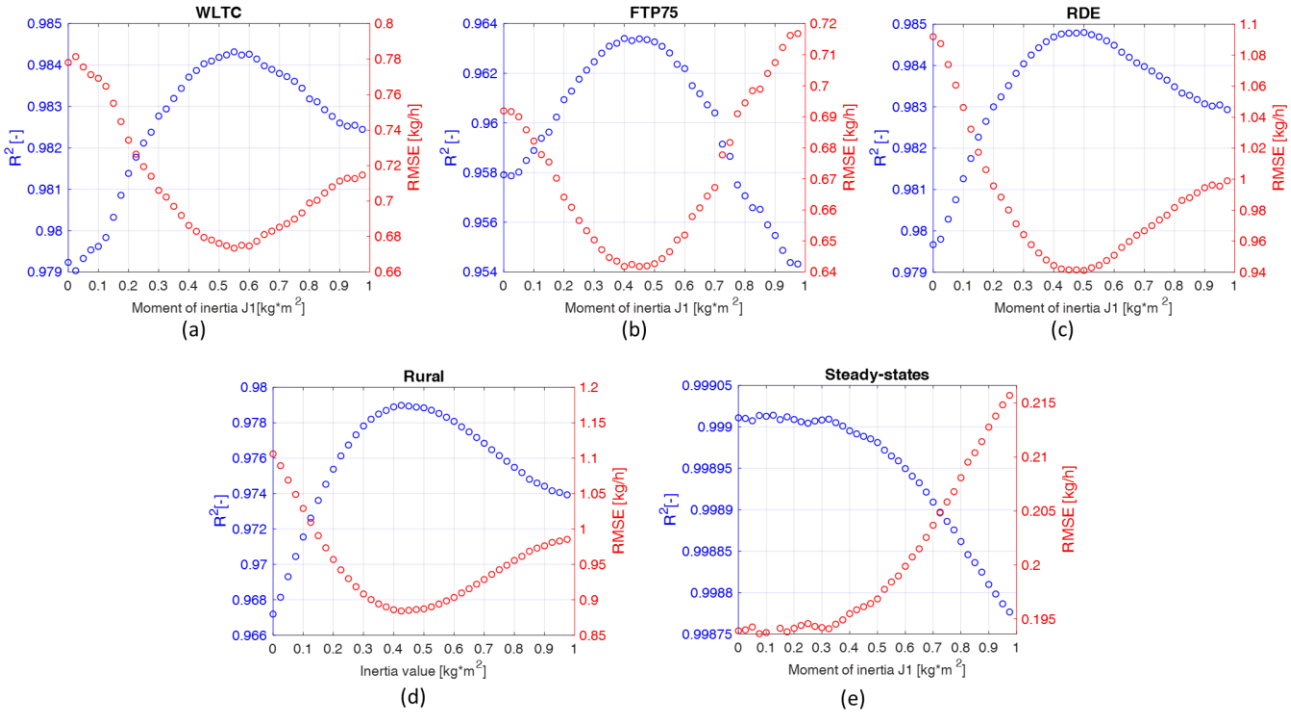

Figure 5: Moment of inertia sensitivity analysis. Variation of RMSE and R^2 as a function of an equivalent moment of inertia along the different driving cycles.

As can be seen, fuel consumption R^2 and RMSE trends show similar shapes with each investigated cycle, demonstrating how the most accurate model performance (corresponding to a maximum in R^2 and minimum in RMSE) is achieved with a J_1 value around 0.45 kg·m^2. The only plot that does not exhibit a maximum in R^2 and minimum in RMSE at around 0.45 kg·m^2 corresponds to the model calibrated (and validated) along the steady-state (SS) dataset. This is legitimate, since this dataset was a sequence of quasi steady-state conditions at different road

gradient and the accelerator pedal position (APP). It is reasonable to believe that no significant improvement should be obtained by incorporating the moment of inertia into the fitting procedure on a dataset with a low transient nature. It should also be noted that, to the authors' knowledge from previous research projects on the engine the tested vehicle is equipped with, this engine has a moment of inertia of approximately 0.3 kg·m^2, so a value of 0.45 kg·m^2 is reasonable, considering that J_1 should represent the equivalent moment of inertia of the entire powertrain, not only of the engine.

The scatter plot in **Figure 6** gives a visual understanding of the prediction accuracy attained by the different models, built without (**Figure 6(a)** and **Figure 6(c)**, for EB models) and with the effect of the moment of inertia of 0.45 kg·m^2 (**Figure 6(b)** and **Figure 6(d)**, for EB* models), calibrated and validated on the RDE (**Figure 6(a)** and **Figure 6(b)**) and Rural (**Figure 6(c)** and **Figure 6(d)**) cycle datasets. The x-axis represents the experimental (measured) fuel consumption values, while the y-axis represents the corresponding predicted values. In addition, R^2, RMSE and Goodness of Fit (GoF) values are reported in the resulting plots, as well as a 45-degree bisector. The 45-degree bisector divides the planes of the plots into two triangular zones of equal size, with data above the reference bisector overestimating and data below underestimating the experimental fuel consumption. The greater the spread of the data around the bisector, the weaker the estimating capabilities of the corresponding models. The statistical parameter defined as Goodness of fit (*GoF*) is evaluated starting from the normalized root mean squared error (NRMSE), calculated using the MATLAB function “goodnessOfFit”, that is based on the following formula:

$$NRMSE = \frac{\|x_{ref} - x\|}{\|x_{ref} - mean(x_{ref})\|} \tag{3}$$

where x_{ref} represents the vector of experimental instantaneous fuel consumption along a generic validation driving cycle and x represents the corresponding instantaneous fuel consumption estimated by a model. This equation is then converted in percentage obtaining a *GoF* value equal to:

$$GoF = (1 - NRMSE) * 100 \quad (4)$$

A *GoF* of 100% means a perfect fit, while 0 represents a straight line matching x_{ref} (bad fit).

As it can be seen, by using a moment of inertia value of 0.45 kg·m^2, R^2, RMSE and GoF are noticeably improved: R^2, RMSE and GoF rise from 0.980, 1.09 kg/h and 85.7% to 0.985, 0.94 kg/h and 87.7% when including the moment of inertia into the fitting process on the RDE dataset, and from 0.967, 1.11 kg/h and 81.9% to 0.979, 0.89 kg/h and 85.5% on the Rural dataset.

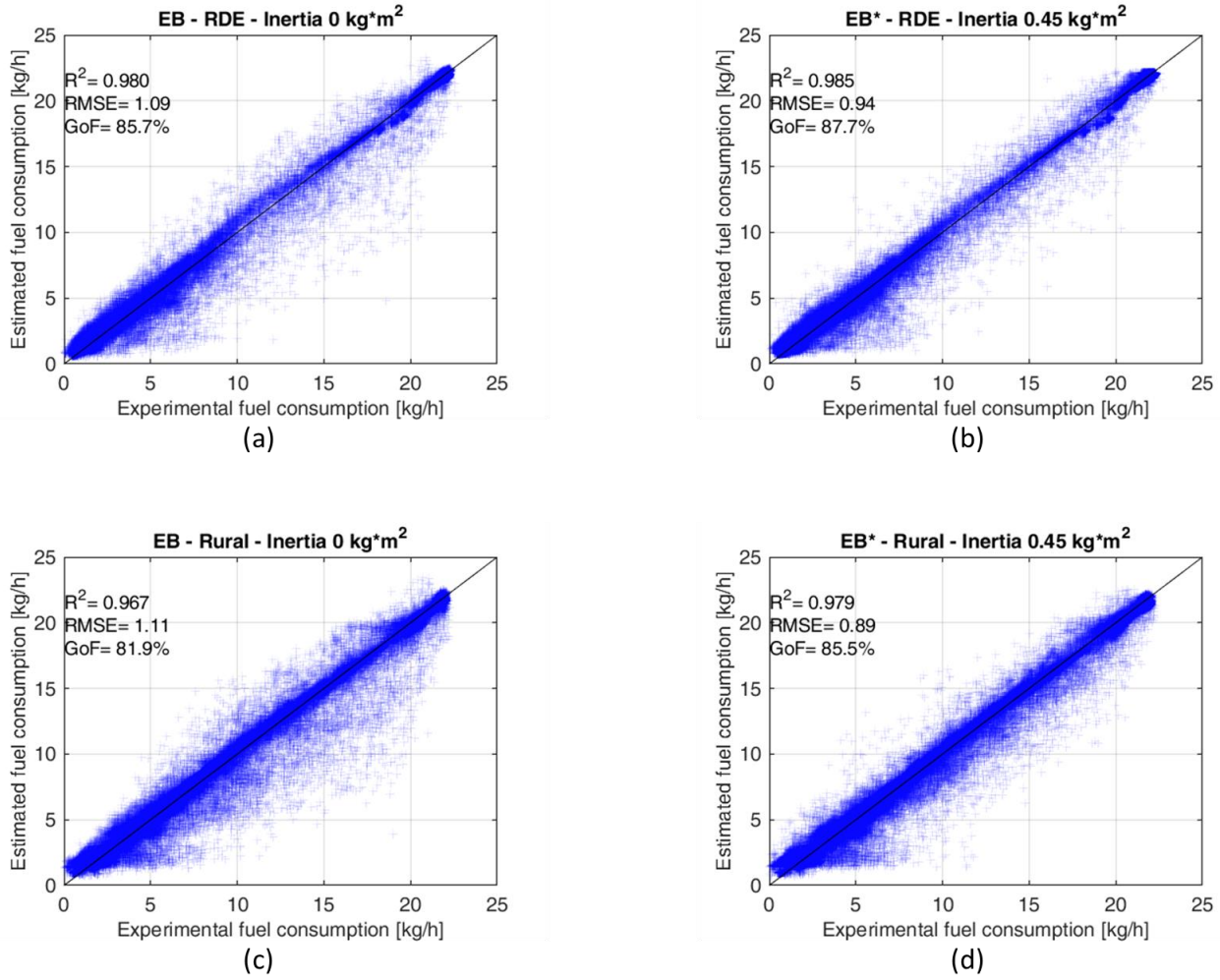

Figure 6: Experimental vs Predicted fuel consumption adopting EB models (without considering the moment of inertia), (a),(c). Experimental vs Predicted fuel consumption adopting EB* models (considering an equivalent moment of inertia value of 0.45 kg·m^2) (b),(d).

4.5. Data handling and synchronization

Before being employed for model calibration, data logging from testbed acquisitions was pre-

processed to ensure robustness and consistency (e.g., the occurrence of missing data, outliers, or any other undesirable phenomenon), which is crucial to ensure reliable results. Furthermore, the synchronization of the various signals was verified. Ensuring the accurate alignment of the measured data is a critical aspect that researchers must always carefully check. For the purpose of this study, in particular, due to the intrinsic correlation between torque and vehicle speed (ultimately, VPD) and fuel consumption, it is logical to assume that a correct signal synchronization (i.e., fuel consumption data properly aligned and consistent with VPD) is key to yield the highest goodness of fit of the resulting models.

Although the fuel consumption measurement device (AVL FuelExact) ensures high measurement accuracy even in transient conditions, the resulting measured fuel flowrate signal may not be perfectly consistent and synchronous with the measured wheel torque and speed signals. The dynamics of the fuel supply circuit from the device and the internal fuel recirculation circuit of the vehicle could both contribute to this signal misalignment, interacting in such a way that they generate complex dynamic effects that are challenging to model. Nevertheless, the main noticeable effect is a delay of the fuel consumption signal relative to the wheel torque and/or speed signals. For this reason, the calibration of all of the models described in the previous Sections was performed after fuel consumption signals were properly advanced by a constant time interval to be synchronous with wheel torque and speed.

Figure 7 visually depicts the abovementioned signal misalignment. It represents a zoomed-in view of a portion of one of the tested driving cycles, where blue lines represent wheel torque (

Figure 7**(a)**) and engine speed (

Figure 7**(b)**) signals, while the black lines represent the original fuel flowrate signal. By comparing these lines, it is evident how, beginning about 522.8 s, there is a sudden rise in both wheel torque and engine speed (due to a driver's accelerator pedal request), which is not followed by an increase in fuel flowrate, as one could expect. Similarly, there is a sudden decline in wheel

torque, with almost steady engine speed, from around 524.7 s, while fuel flowrate keeps increasing. These behaviours are definitely not physical and most likely caused by a lack of correct signal synchronization. For this reason, red lines were added to both plots, representing the same fuel flowrate signal advanced by 0.4 s; this way, fuel consumption data are much more correlated with wheel torque and engine speed. Similar behaviours could be found across all experimental datasets, and a 0.4-s advance seemed to be the best compromise.

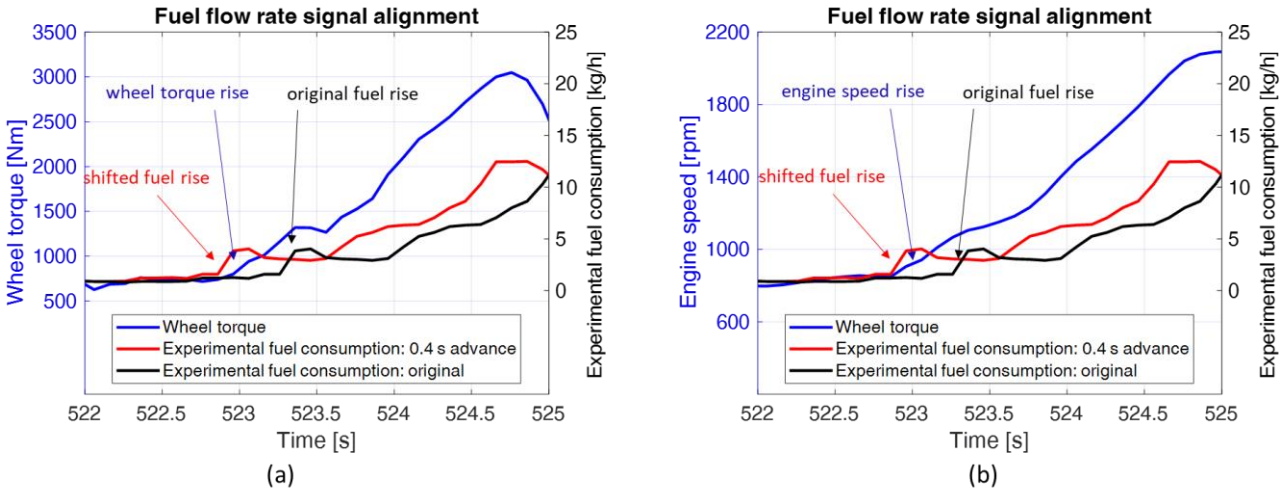

Figure 7: Zoomed part of RDE cycle to highlight fuel disalignment. Black line represent the raw fuel measurments. Blu line represent indicative vehicle parameters (wheel torque on the left, engine speed on the right). Red line represent the original fuel advanced of 0.4 s in order to align the rise in fuel to the rise in engine speed and wheel torque.

In order to verify whether the 0.4 s advance was really optimal, and to further emphasize the need of this fuel data shift, a sensitivity analysis was carried out by calibrating different tentative models upon the same experimental dataset (the RDE dataset, for example) and either advancing or delaying the fuel flowrate data within a ±1-s interval, with 0.1-s steps. The accuracy of these tentative models was then assessed on the same dataset they were calibrated upon and, as previously done, RMSE and R^2 values were used to assess their fitting performance. Specifically, 20 tentative models were calibrated (and validated) upon the RDE dataset. **Figure 8** depicts the results in terms of RMSE (**Figure 8(a)**) and R^2 (**Figure 8(b)**) as a function of the fuel consumption shift (negative

values indicate an advance, positive values a delay). The blue lines refer to EB* models, while the red lines correspond to VB models.

It is evident that optimal outcomes in terms of R^2 and RMSE are achieved when the shift values are set to -0.3 ÷ -0.4 s, with negligible differences coming from adopting EB* or VB approaches. A 0.4-s advance was thus employed for all the experimental datasets dealt with in this study.

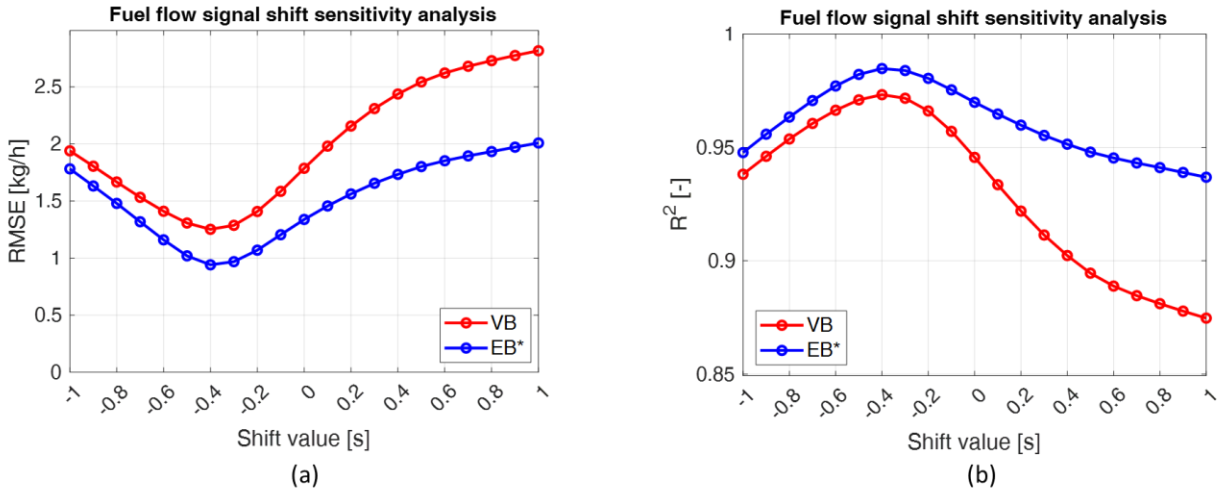

Figure 8: Fuel shift sensitivity analysis. RMSE (a) and R^2(b) calibrating and validating different tentative VB models (that use vehicle-based coordinate) and different tentative EB* models (that use engine coordinates considering a moment of inertia value of 0.45 kg·m^2) shifting the raw fuel consumption data of ±1 second with steps of 0.1 second.

5. Results and discussion

5.1. Cross-validation

After discussing how three different approaches to build models for fuel consumption estimation are possible (VB, EB, EB*), and describing the preliminary activity performed to properly set up data and models, this Section delves deeper into the accuracy differences between the three proposed strategies. To do so, for each of the three proposed modeling approaches, a total of six different model calibrations were carried out, using the six available experimental datasets (WLTC, FTP-75, Rural, RDE, SS and Joined, cf. **Figure 3**). Then, every model calibration was cross-

validated with respect to all the available driving cycles, assessing their accuracy through *GoF* (as defined in **Equation (4)**) and cumulative fuel consumption errors (FC_d). The cumulative fuel consumption error, is evaluated by computing the relative difference between the integral of the instantaneous fuel consumption estimated by model ($\int \dot{m}_{f,estimated}(t)\,dt$) and that experimentally measured ($\int \dot{m}_{f,exp}(t)\,dt$):

$$FC_d = \frac{\int \dot{m}_{f,estimated}(t)\,dt - \int \dot{m}_{f,exp}(t)\,dt}{\int \dot{m}_{f,exp}(t)\,dt} \tag{5}$$

Cross-validation results are shown as bar plots in **Figure 9**. The bar colours show which calibration cycle the results refer to, while the bar groups on the x-axis represent the validation cycle. For every colour, overlapped bars with different shades and thickness represent the results obtained with the three considered models (VB, EB, EB*). In particular, the thickest and most transparent bars refer to VB, the thinnest and most opaque bars refer to EB*, while the mid-thickness and mid-transparency bars refer to EB.

As an example, the black overlapped bars included in the first set of bars labelled “WLTC” in **Figure 9(a)** and **Figure 9(b)** represent *GoF* values and FC_d, respectively, obtained by validating on the WLTC cycle the models (VB, EB, EB*) calibrated on the RDE cycle dataset. To better recognize the bars that represent the results in training/calibration for every considered model, a “C” symbol was added on top of each corresponding bar.

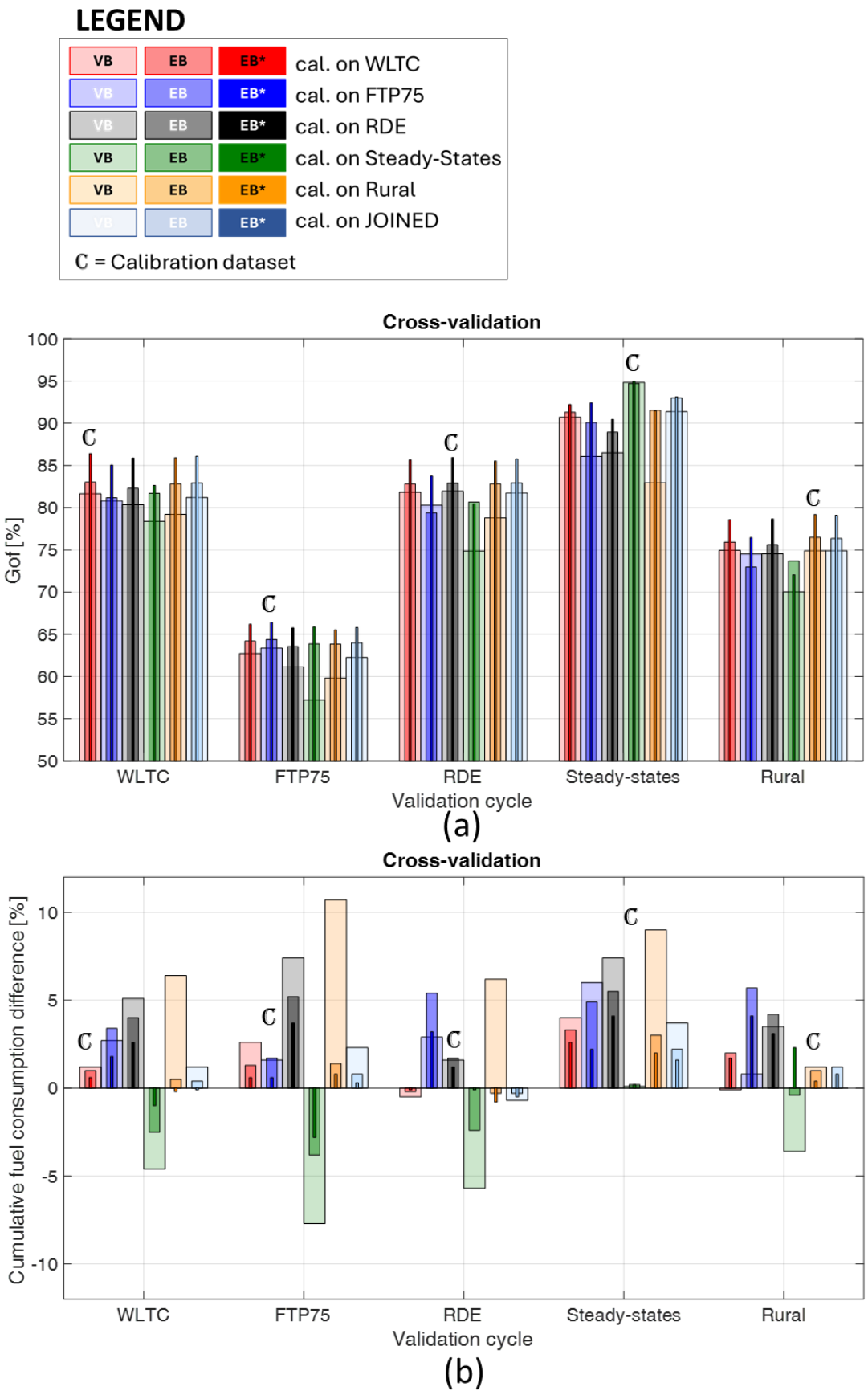

Figure 9: *GoF* (a) and FC_d(b) along the cross-validation. Bar colors represent the calibration cycle i.e the cycle that has been used to calibrate the tentative model, as reported in the legend. Thikness

and shadness represent the model type. Thick and transparent bar repsesent VB models, thin and dark represent EB* models while EB models are represented by middle thikness and trasparency. X-axis label define the validation cycle.

The main observations that can be made from **Figure 9** are reported hereinafter.

- In **Figure 9(a)**, the first noteworthy difference that stands out is how, by switching from a vehicle-based (VB, cf. the thickest and most transparent bars) to an engine-based model (EB, cf. the intermediate-thinness and more opaque bars), bar heights tend be more uniform, which means more consistent (and, in general, higher) model accuracy, as defined in terms of *GoF* values. This enhancement in estimating consistency and accuracy, achieved by switching from VB to EB, can be ascribed to the fact that the engine-based inputs required by EB models are inherently more correlated with fuel consumption than vehicle-based inputs required by VB models. For a given wheel speed and wheel torque, in fact, multiple engine operating points may be possible, depending on the instantaneous gear engaged. Moreover, each of these engine operating points may exhibit markedly different efficiency and, thus, markedly different fuel consumption. Differences that may be greatly reduced when the experimental points to be fitted are represented as a function of engine coordinates: this way, every engine operating point is, in theory, inherently associated with a unique fuel consumption value, thus possibly showing a cleaner distribution of the experimental points relative to their engine-based domain. This allows for improved quality of the fitting process which results in greater independence of the estimating results with respect to the calibration cycle. Similar improvement can be detected also from **Figure 9(b)**: there is a general reduction in FC_d switching from VB to EB models.
- In the same **Figure 9(a)**, an additional fitting improvement seems to be achievable by further switching from EB to EB* (engine-based model taking into account the effect of powertrain moment of inertia), evidenced by the fact that the thinnest and most opaque bars related to EB* are nearly always the tallest (i.e., highest *GoF* values). This is true regardless

of the particular experimental dataset used for model calibration. A significantly lower FC_d can be also highlighted for EB* models in **Figure 9(b)**: most of the bars related to them are bounded in a range of ±2% , with the worst spikes (up to +4.1%) occurring when validating the model calibrated using RDE on the SS dataset, most likely due to the different transient nature of these two cycles.

- Models calibrated on the Joined dataset are the ones giving the best estimating results (i.e., high GoF, low FC_d), regardless of the particular modelling approach (VB, EB or EB*). This could be partly attributable to the fact that validation is carried out on a subset of the data already included in the calibration dataset, since the Joined dataset includes all of tested driving cycle.
- Interestingly, EB* tends to show good estimating performance (i.e., high GoF, low FC_d) on all validation datasets regardless of the particular dataset used for model calibration, in contrast to VB model, whose calibration datasets affect to a greater extent the final estimating outcome. This confirms the superior physical significance of EB* model that, despite some degree of increase in complexity, gives far more accurate fuel consumption estimations even when validated on datasets that are different from the calibration one. Nevertheless, the estimating accuracy is still more than acceptable even with the simplest VB modelling approach.

5.2. Additional benefits of switching from a VB to an EB domain

Additional benefits resulting in switching from vehicle-based to engine-based inputs may arise in some cases where the vehicle speed and torque domain is not fully explored by the calibration dataset. For example, this happens when considering the calibration of a VB model on the Rural dataset and its validation on the RDE dataset.

As a matter of fact, the vehicle velocity profile of the Rural driving cycle is limited to 120 km/h. This means that any attempt to validate a VB model on a cycle like the RDE, which reaches

vehicle velocity values up to around 150 km/h, would produce unavoidable extrapolation errors when trying to estimate the fuel consumption from the vehicle travelling faster than 120 km/h. **Figure 10(a)** displays the instantaneous fuel consumption estimated by a VB model calibrated on the Rural dataset (orange line) and the experimental instantaneous fuel consumption (black line) along a portion of the RDE cycle where the vehicle travels faster than 120 km/h. It is evident that this VB model extrapolates values incorrectly, resulting in a final +6% FC_d, as reported in **Figure 9(b)**.

In cases like this, bad extrapolation issues can be resolved by switching from a vehicle-based to an engine-based domain. As evidence of that, the distributions of the experimental points along the Rural dataset are displayed on a vehicle-based domain (n_{wheel}, T_{wheel}), in **Figure 10(c)**, and on an engine-based domain (n_{eng}, T_{eng}), in **Figure 10(d)**. Comparing these two Figures, it is clear that just switching from a vehicle-based to an engine-based domain transforms the Rural dataset from a collection of samples with an entire portion of the domain unexplored to a corresponding dataset where the distribution of samples is wide enough to cover much better the entirety of the engine-based domain. By doing so, when an EB* model (instead of a VB) is calibrated on the Rural dataset and validated on the RDE cycle, as shown in **Figure 10(b)**, fuel consumption estimations are much better. In this case, the orange line is remarkably closer to the experimental black line, even in the portions of the RDE cycle where the vehicle travels faster than 120 km/h. This positive outcome is also reflected in the great reduction in FC_d that EB* model gives compared to the corresponding VB, as evidenced by **Figure 9(b)**: looking at the orange bars for the x-axis group labelled “RDE”, the thinnest bar (corresponding to the EB* model) is remarkably lower than the thickest one (corresponding to the VB model).

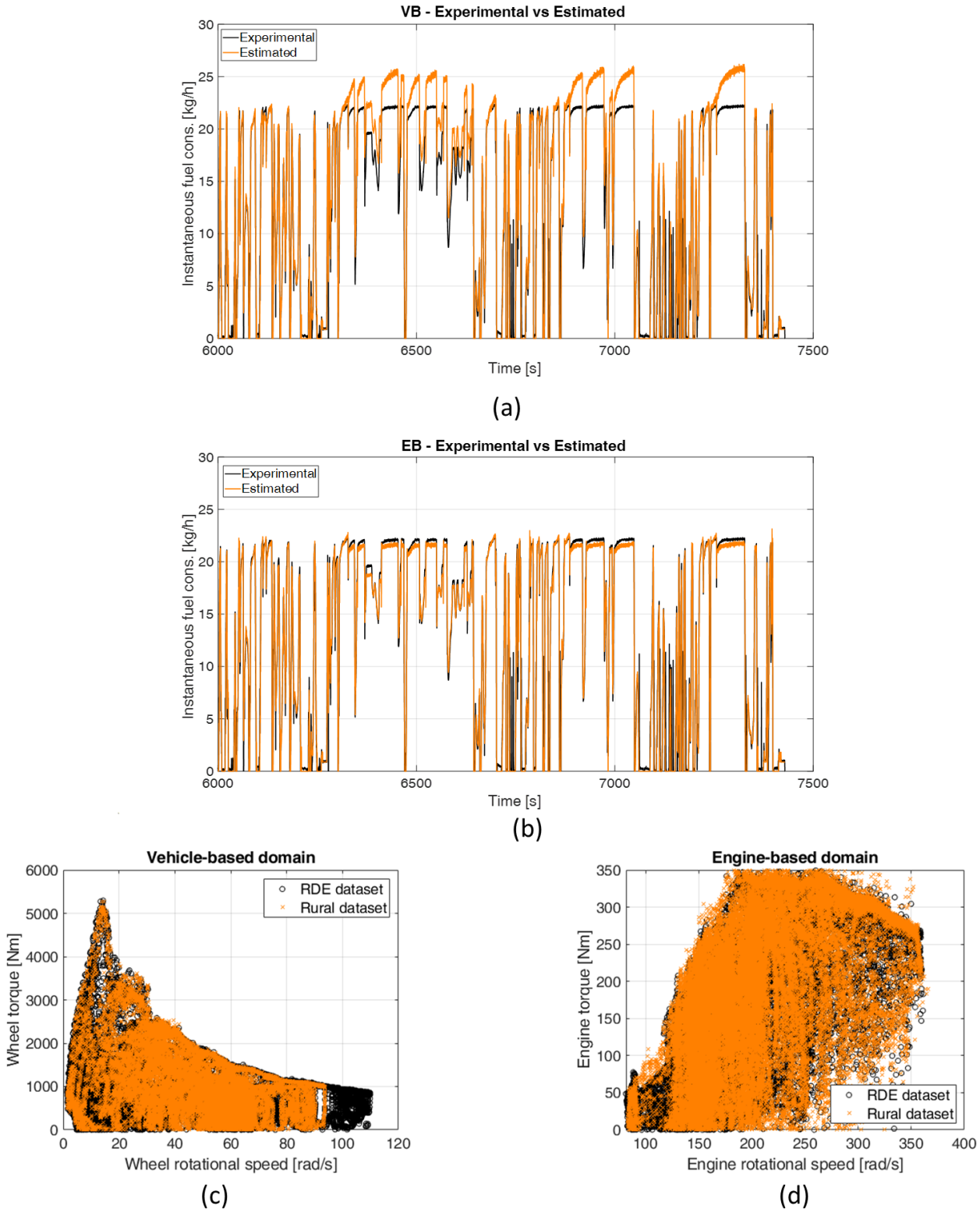

Figure 10: Experimental vs predicted instantaneous fuel consumption along a part of RDE cycle. Fuel predicted by VB model (a) and EB model (b). Representation of engine points explored in the RDE (black) and Rural (orange) cycles in the vehicle-domain (c) and engine domain (d)

5.3. Instantaneous fuel consumption for VB, EB and EB models*

Finally, an illustration of the instantaneous fuel consumption, both experimental and estimated (by VB, EB, EB* models), is given below along the portion of a WLTC cycle, to show the reader a concrete example of the prediction accuracy achieved with the three different modelling approaches.

The experimental fuel consumption is shown in blue across all subplots in **Figure 11**, while the instantaneous fuel consumption estimated by the different models (all of which were calibrated on the Joined dataset, since it is, as illustrated earlier, the dataset that yields the most accurate and uniform results for all the three considered modelling approaches) are depicted in red for the VB model (**Figure 11(a)**), in green for the EB model (**Figure 11(b)**) and in black for the EB* model (**Figure 11(c)**). In general, prediction accuracy is rather good for all the three considered models. One notable difference, though, is that the EB* model, which takes into consideration the powertrain moment of inertia, better estimates fuel consumption during rapid acceleration/deceleration phases and during gearshifts as well (see the last portion of the cycle depicted in **Figure 11**: experimental fuel consumption "valleys" are estimated much better by the EB* model, compared to the other two models).

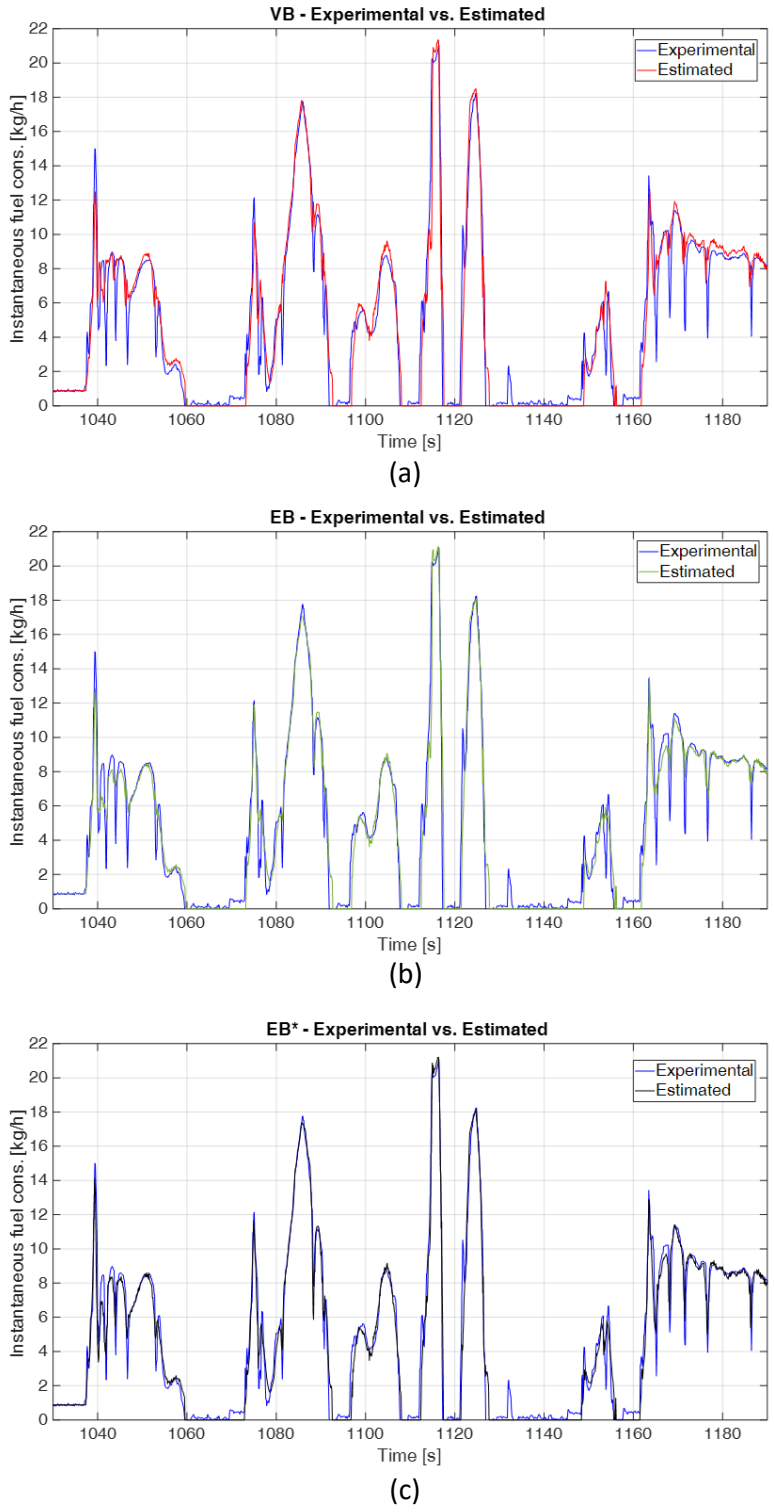

Figure 11: Measured vs estimated fuel consumption along a portion of the WLTC cycle. Prediction done with models calibrated on Joined dataset. (a) VB model, (b) EB model, (c) EB* model

Summary and conclusions

This paper investigates a methodology for building simple instantaneous fuel consumption models

of a diesel-powered vehicle based on a small set of transient experimental data collected on a four-dyno vehicle/powertrain testbed. The procedure relies on vehicle-level black-box approach and a locally weighted linear regression method, to address the limitations of more conventional approaches based on steady-state engine maps (that need to be couple with additional, and rather detailed, models of the other sub-systems of the vehicle driveline) or machine learning (that usually requires high computational power).

Specifically, the paper describes the development of three different modelling approaches (namely VB, EB and EB*) with the goal of constructing simple and fast-to-build models for estimating the instantaneous vehicle energy consumption through locally weighted linear regression, without resorting to detailed modeling of the vehicle, which can be complex to implement at times, due to the absence of specific technical data about the vehicle itself.

Starting from experimental tests carried out at the CARS vehicle and powertrain testbed (Politecnico di Torino) on a conventional diesel-powered vehicle, data analysis was performed to synchronize, clean, and align the data, first. Then, different models were built, beginning with the simplest vehicle-based (VB) model, which is able to estimate fuel consumption by merely using wheel torque and speed as inputs. The VB model has the benefit of requiring inputs that are directly measured from the testbed dynos or, in the case of simulation, simply obtained through longitudinal dynamics vehicle equations, adopting vehicle coast-down coefficients to estimate wheel torque values.

Next stage was to create a variation of the VB model with the goal of improving its accuracy. The initial step was to switch to engine-based coordinates, which are intrinsically more correlated with engine operation and, thus, fuel consumption. This way, the EB model was obtained. It requires engine speed and torque as inputs, as well as transmission-related parameters (e.g., gear ratio, current gear engaged, etc.). Besides the slight increase in complexity compared to the VB model, a good improvement in estimation accuracy was highlighted.

Third stage was then to create a variation of the EB model, thus obtaining a third model (the EB* model) that also took into account the moments of inertia of the rotating parts of the powertrain. If no information is available about their values, a methodology was proposed to estimate an equivalent moment of inertia, by means of a numerical sensitivity analysis. Again, at the expense of a supplemental increase in model complexity, albeit slight, a further improvement in estimation accuracy was highlighted.

Finally, a thorough cross-validation comparison of the accuracy of these three modelling approaches revealed the advantages and disadvantages of each technique.

The approach described in this paper can be an important tool for developing and evaluating eco-driving or ADAS functions, as well as for comparing energy consumption between vehicles that were not tested on the same driving cycle. However, these black-box vehicle-level models are only applicable to one vehicle configuration at a time. If the vehicle configuration is changed (e.g., engine or any driveline component), the fitting procedure must be recalibrated for the new vehicle configuration. This indicates that the proposed approach is particularly appropriate in case of newly developed vehicle strategies, such as eco-driving and eco-routing systems, or for energy consumption evaluation of same-vehicle fleets. These fuel consumption models can also provide a better assessment of the use-phase energy consumption of a vehicle for LCA (Life-Cycle Assessment) analysis: instead of evaluating the energy consumption of a vehicle based on official type-approval fuel consumption data, a much more reliable assessment could be made using these more reliable fuel consumption models on appropriate mission profiles, without the need of purposely dedicated experimental campaigns. Finally, future work will be carried out to demonstrate how the approach described in this paper can be extended to model the instantaneous power consumption of electric vehicles, as well.

Nomenclature

ADAS	Advanced Driver Assistance System
ANN	Artificial neural network

APP	Accelerator pedal position
CARS	Center for Automotive Research and Sustainable mobility
EB	Engine-based
EB*	Engine-based modified (including the effect of the powertrain moment of inertia)
ECU	Electronic control unit
EM	Electric motor
FC_d	Cumulative fuel consumption difference/error
FTP-75	Federal Test Procedure
GoF	Goodness of fit
ICE	Internal combustion engine
J_1	Moment of inertia corresponding to the masses rotating at engine speed
J_2	Moment of inertia corresponding to the masses rotating at wheel speed
LCA	Life-cycle assessment
LSTMs	Long short-term memory neural networks
$\dot{m}_{f,estimated}$	Estimated fuel flowrate by model
$\dot{m}_{f,exp}$	Experimental fuel flowrate from testbed measurement device
n_{engine}	Engine rotational speed
NRMSE	Normalized root mean square error
n_{wheel}	Wheel rotational speed
OBD	On-board diagnostics
R^2	Coefficient of determination
RDE	Real driving emissions
RMSE	Root mean square error
SS	Steady states
t	time
T_{engine}	Engine torque
T_{wheel}	Wheel torque
VB	Vehicle-based
VPD	Vehicle power demand
WLTC	Worldwide harmonized light vehicles test cycle
τ_{fd}	Final drive ratio
τ_{gear}	Engaged gear ratio

Acknowledgments

Omar Marello acknowledges MICS (Made in Italy –Circular and Sustainable) Extended Partnership for receiving funding from the European Union Next-Generation EU (PIANO NAZIONALE DI RIPRESA E RESILIENZA (PNRR) – MISSIONE 4 COMPONENTE 2, INVESTIMENTO 1.3 – D.D. 1551.11-10-2022, PE00000004).

References

[1] Favelli S, Castellanos Molina LM, Mancarella A, Marello O, Tramacere E, Manca R, et al. Fuel Economy Assessment of MPC-ACC on Powertrain Testbed, 2024, p. 826–32. https://doi.org/10.1007/978-3-031-70392-8_117.

[2] Saerens B, Rakha H, Ahn K, Van Den Bulck E. Assessment of Alternative Polynomial Fuel Consumption Models for Use in Intelligent Transportation Systems Applications. J Intell Transp Syst 2013;17:294–303. https://doi.org/10.1080/15472450.2013.764801.

[3] Zeng W, Miwa T, Morikawa T. Eco-routing problem considering fuel consumption and probabilistic travel time budget. Transp Res D Transp Environ 2020;78:102219. https://doi.org/10.1016/j.trd.2019.102219.
[4] Zhou M, Jin H, Wang W. A review of vehicle fuel consumption models to evaluate eco-driving and eco-routing. Transp Res D Transp Environ 2016;49:203–18. https://doi.org/10.1016/j.trd.2016.09.008.
[5] Kanarachos S, Mathew J, Fitzpatrick ME. Instantaneous vehicle fuel consumption estimation using smartphones and recurrent neural networks. Expert Syst Appl 2019;120:436–47. https://doi.org/10.1016/j.eswa.2018.12.006.
[6] Yang Y, Gong N, Xie K, Liu Q. Predicting Gasoline Vehicle Fuel Consumption in Energy and Environmental Impact Based on Machine Learning and Multidimensional Big Data. Energies (Basel) 2022;15:1602. https://doi.org/10.3390/en15051602.
[7] Ren S, Li T, Li G, Liu X, Liu H, Wang X, et al. Investigation of Heavy-Duty Vehicle Chassis Dynamometer Fuel Consumption and CO2 Emissions Based on a Binning-Reconstruction Model Using Real-Road Data. Atmosphere (Basel) 2023;14:528. https://doi.org/10.3390/atmos14030528.
[8] Ehmer M, Khan F. A Comparative Study of White Box, Black Box and Grey Box Testing Techniques. International Journal of Advanced Computer Science and Applications 2012;3. https://doi.org/10.14569/IJACSA.2012.030603.
[9] Chen L, Hu M, Wang D, Wang H, Li W, Qin D. Polynomial-based model for estimating instantaneous fuel consumption. Proceedings of the Institution of Mechanical Engineers, Part D: Journal of Automobile Engineering 2023;237:2872–84. https://doi.org/10.1177/09544070221116184.
[10] Chiara F, Wang J, Patil CB, Hsieh M-F, Yan F. Development and experimental validation of a control-oriented Diesel engine model for fuel consumption and brake torque predictions. Math Comput Model Dyn Syst 2011;17:261–77. https://doi.org/10.1080/13873954.2011.562902.
[11] Lindgren M. A Transient Fuel Consumption Model for Non-road Mobile Machinery. Biosyst Eng 2005;91:139–47. https://doi.org/10.1016/j.biosystemseng.2005.03.011.
[12] Bohbot J, Miche M, Pacaud P, Benkenida A. Multiscale Engine Simulations using a Coupling of 0-D/1-DModel with a 3-D Combustion Code. Oil & Gas Science and Technology - Revue de l'IFP 2009;64:337–59. https://doi.org/10.2516/ogst/2009007.
[13] Rui D, Hui J. High-accuracy transient fuel consumption model based on distance correlation analysis. Fuel 2022;321:123927. https://doi.org/10.1016/j.fuel.2022.123927.
[14] Ahn K, Rakha H, Trani A, Van Aerde M. Estimating Vehicle Fuel Consumption and Emissions based on Instantaneous Speed and Acceleration Levels. J Transp Eng 2002;128:182–90. https://doi.org/10.1061/(ASCE)0733-947X(2002)128:2(182).
[15] Mortabit I, Rachid A, Errifai N, Khamlichi S, Saidi E, Mazouzi A El, et al. Instantaneous Vehicle Fuel Consumption Estimation Using Neural Networks, 2024, p. 702–13. https://doi.org/10.1007/978-981-97-0126-1_62.
[16] Moradi E, Miranda-Moreno L. Vehicular fuel consumption estimation using real-world measures through cascaded machine learning modeling. Transp Res D Transp Environ 2020;88:102576. https://doi.org/10.1016/j.trd.2020.102576.
[17] Meng X, Pang K, Di B, Li W, Wang Y, Zhang J, et al. Road grade estimation for vehicle emissions modeling using electronic atmospheric pressure sensors. Front Environ Sci 2023;10. https://doi.org/10.3389/fenvs.2022.1051858.